Natural Hazards **25:** 23–35, 2002.

The Role of Earthquake-Related Effects in Urban Complexes

E. L. LEKKAS
Department of Geology, University of Athens, Panepistimioupoli, Athens 15784, Greece
Tel.: (+301) 7274410; Fax: (+301) 6845061; e-mail: elekkas@geol.uoa.gr

(Received: 2 February 2000; in final form: 19 September 2000)

Abstract. A number of cases where earthquake-induced damage was massive or presented interesting distribution patterns in recent earthquakes are presented. The highly serious damage along reactivated seismic faults and fractures is discussed for the earthquakes of Pyrgos (Greece), Egio (Greece) and Kobe (Japan). Additionally, we describe characteristic types of building failure in the earthquake of Egio, caused by the coexistence of surficial faulting and liquefaction. Of particular interest is the damage pattern in the Kobe and Dinar earthquakes, attributed to seismic wave directivity, caused by migration of the earthquake source. Finally, a special case of building damage is described for the case of the Adana, Turkey earthquake, which is connected to the shape and the azimuthal location of buildings in respect to the epicentre. All the above cases are valuable sources of information and can be utilized in the reduction of seismic risk in constructions and urban complexes.

Key words: earthquake design, damage distribution, liquefaction, earthquake faulting, seismic wave directivity

1. Introduction

Microzonation studies are nowadays globally accepted as the most reliable approach towards the earthquake-proof design of urban complexes and the reduction of seismic risk. For the compilation of such studies, the approach has to be multidisciplinary, as a large number of data have to be taken into account, including *in situ* measurements, results of laboratory tests, numerical modelling, evaluations and cross-checking of data.

In spite of the fact that there has been a broadly accepted platform for the implementation of such a methodology, the subject of microzonation studies is yet to be fully developed, as new data are continually added to the existing know-how. These are mainly taken from evaluation of earthquake recordings, after events that hit urban complexes, and gradually allow us to reshape our attitude towards earthquake-proof planning, with the ultimate goal of the further reduction of seismic risk.

The following paragraphs deal with cases of unusual earthquake-induced damage at man-made constructions and urban complexes.

The following paragraphs include a number of unusual earthquake-induced damage at various construction types, as well as special damage distribution patterns, observed in recent earthquakes. The earthquakes on which we shall focus are the following, in chronological order:

- **Pyrgos earthquake (26 March 1993, Greece).** The magnitude and focal depth of this event were Ms = 5.2 and h = 10 km, respectively. Its epicentre was located at the NE outskirts of the town of Pyrgos (W. Peloponnessos). The earthquake resulted in heavy damage within the town, where 50% of the buildings were affected. Damage also spread across the broader area, while a series of geological site effects, as landslides and liquefaction also took place.
- **Kobe earthquake (17 January 1995, Japan).** This great event (Ms = 7.2) caused the death of several thousands of people and the demolition of extended parts of the Kobe–Osaka urban complex. A large surface rupture on Awaji Island (Nojima fault), trending NE-SW was observed and a suite of disastrous site effects occurred, all exacerbating the already grave consequences of the shock.
- **Egio earthquake (15 June 1995, Greece).** This shock measured 6.1 on the magnitude scale (Ms), while its focus lay at a depth of approximately 15 km. A large number of people were killed and the urban and surrounding areas of Egio were severely hit. Among the surficial expressions of the tremor were a E-W trending rupture and a series of geological and geomorphological effects as liquefaction, landslides, land settlement and coastline retreat, all with significant consequences on constructions.
- **Dinar earthquake (1 October 1995, Turkey).** Its magnitude was Ms = 6.1 while its focal depth was estimated between 8 and 15 km. It was caused by the reactivation of a NW-SE trending normal fault. One hundred people were killed in the city of Dinar and the vicinity. In Dinar alone, over 65% of buildings suffered significant damage.
- **Adana earthquake (27 June 1998, Turkey).** The most recent earthquake in this list had a magnitude Ms = 6.2 and a focal depth in the range of 10–20 km. It killed about 150 people and damage was spread in the broader area of the city of Ceyhan, which was the most severely hit urban complex. Ceyhan is located 45 km NE of the epicentre, almost along the trace of a NE-SW trending reactivated oblique-slip fault (normal with significant left-lateral strike slip component).

The following sections outline the earthquake-related effects and their influence on the occurrence of accumulated damage and its unusual distribution patterns during the aforementioned earthquakes.

2. Surficial Faulting

Shallow earthquakes have often resulted in dramatic intensity increase along the surficially reactivated faults and fault zones; such representative examples can be

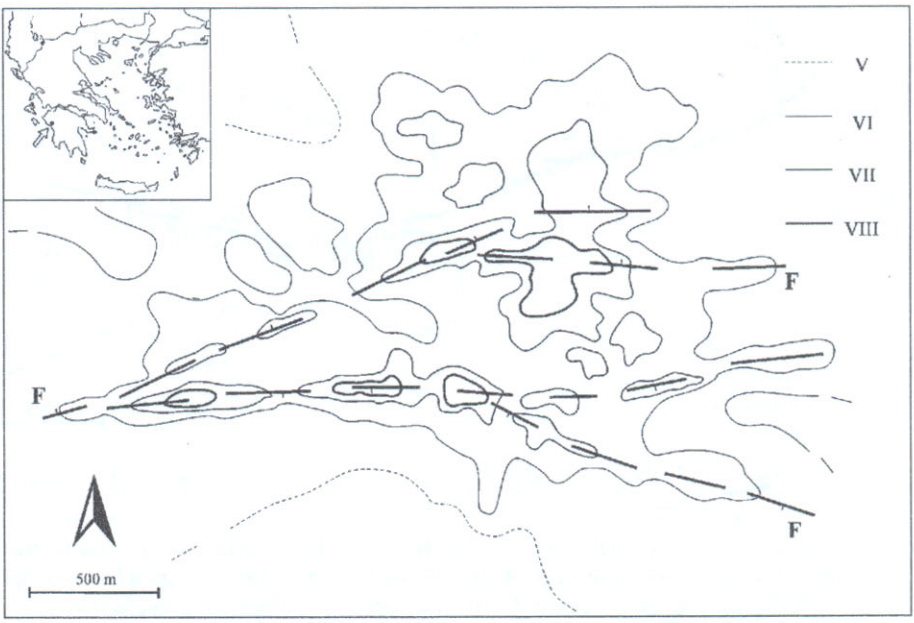

Figure 1. Intensity distribution (I_{EMS92}) in the town of Pyrgos for the 26 March 1993 earthquake. Intensity is clearly increased along the traces of the reactivated faults (F). Note also the elongated form of VII and VIII isoseismals.

found in the Pyrgos, Egio, and to some extent, in the Kobe earthquakes. Specifically, during the Pyrgos earthquake, intensity was significantly increased along the two E-W trending active faults that cross the town (Figure 1). The isoseismal contours drawn at the vicinity of these faults were clearly elongated along the E-W direction. Intensities along the faults reached I_{EMS92} = VII and locally VIII. In the remainder of the urban area the recorded intensities were I_{EMS92} = V–VI. It should also be noted that light to medium structural damage to reinforced concrete (R/C) frame buildings was observed along the traces of the reactivated faults (Lekkas, 1996). The affected buildings include public facilities, such as the city hospital and schools, all built to meet the requirements of the National Earthquake-proof Building Code.

Similar was the picture at the Egio earthquake. The E-W trending reactivated fracture was parallel to the graben of the Gulf of Korinthos, marked a portion of the coastline and ran through the town of Egio. The town itself and the surrounding area were damaged, but the most severe cases were observed at ten earthquake-proof R/C frame buildings founded approximately on the trace of the 2 km-long reactivated fracture (zone A in Figure 2). The geometrical and kinematic characteristics of the fracture were similar to those of the earthquake fault mechanism. Two R/C multi-story buildings located on its trace collapsed, while partial collapse and significant damage was recorded at other modern buildings, both R/C and masonry (Figure 2). Meanwhile, damage was scattered throughout the rest of the town (zone

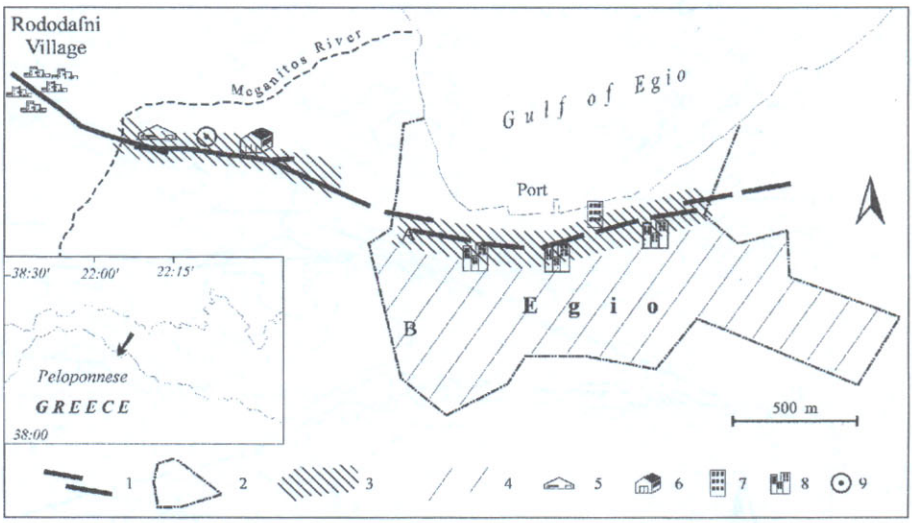

Figure 2. Damage distribution in the 13 June 1995 Egio earthquake. 1. Seismic fracture. 2. Town limits. 3. Zone A (see text). 4. Zone B (see text). 5. Hellenic Weapon Industry. 6. Factory. 7. Collapsed apartment block. 8. Condemned apartment blocks. 9. Liquefaction.

B in Figure 2) and was severe at old buildings that did not meet any earthquake design standards (Lekkas *et al.*, 1996b, 1997).

In the case of Kobe, the relationship between surficial faulting and damage distribution seems at first less straightforward. The reactivated fault zone was identified as the Rokko Fault Zone (RGAFJ 1991, Sato *et al.*, 1995), which comprises numerous segments, with an average NE-SW strike, and its southwestern prolongation that includes the reactivated Nojima fault on Awaji Island (Figure 3). Surficial faulting on the island was impressive, with offset as much as 1.5 m (dextral) and 1.3 m (dip-slip component). On the northeastern prolongation of the Nojima faults, in the Akashi straits, between the island and the mainland, marine seismic survey conducted after the earthquake located reactivated fault segments, one of them having offset the two main towers of the Akashi bridge as much as 1.1 m (EERC, 1995). Within the straits, the fault zone was found to step over to two other segments, both reactivated in the Hanshin earthquake (Sommerville, 1995). The northward onshore prolongation of these segments was located in western Kobe. A post-earthquake relevelling survey in this site showed that onshore differential displacement across them was 26 cm (EERC, 1995). East of Kobe, several reactivated fault strands were found (EERC, 1995); these strands belong to the Arima-Takatsuki fault, which is the northeastern member of the Rokko fault zone. However, direct evidence for surficial faulting within Kobe has remained elusive; building coverage may have obscured the indications for abrupt surficial deformation within the city. Notwithstanding, the aftershock distribution and the clearly elongated shape of the XI-X isoseismal contours (Lekkas *et al.*, 1996a) are clearly indicative of the reactivated fault zone. The fact is that the heavy damage belt is

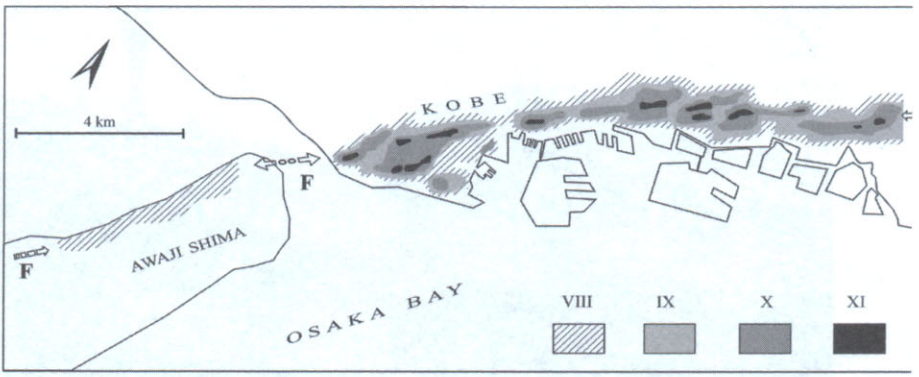

Figure 3. Intensity distribution (I_{EMS92}) for the 17 January 1995 Kobe earthquake, marked by the elongated form of the isoseismals of the prolongation of the reactivated Nojima fault (F).

offset from the postulated fault trace, by a few hundreds of m to 1 km (Kohketsu, 1995). Extensive research has shown that this is attributable to the 'basin edge' or 'bump' effect (Takemiya and Adam, 1995; Kawase, 1996; Kawase *et al.*, 2000 and many others). Hence, it can be said that although direct proof for surficial faulting within Kobe – but it is clear for its environs – has not come to light, it is clear that the heavily damaged narrow belt ran very close and parallel to the mapped active fault zone, which displayed surficial faulting in suburban and rural areas.

3. Earthquake Faulting and Liquefaction

Both earthquake faults and liquefaction are crucial factors to the occurrence of damage. The consequences can be far more severe when these two factors co-exist. Such cases are not frequent and call for the contribution of a number of parameters. Included in this paper is one case with such conditions, namely the Egio earthquake, where the consequences on constructions were grave.

In the Egio earthquake, a series of liquefied sites were observed along the surficial fracture, especially close to the western extremity of it (Carydis *et al.*, 1995a; Lekkas *et al.*, 1996b, 1998). One such example was the partial collapse of the building of the Hellenic Weapon Industry, a two-storey earthquake-proof R/C frame construction located only a few meters away from the fracture, along which liquefaction was observed (Figure 2). Parts of the building collapsed totally, while others suffered heavy structural damage (Figure 4). Besides, a number of other buildings located on the fracture also collapsed or had heavy structural damage, too.

Figure 4. Collapse of industrial buildings, built to meet high earthquake design standards, and founded close to the surficial expression of seismic fractures and liquefaction.

4. Directivity of Seismic Waves

Clear phenomena of seismic wave directivity in recent earthquakes were observed in the Kobe and Dinar earthquakes. In the Kobe event, the prolongation of the NE-SW trending fault on Awaji Island was within the Kobe urban complex. The fault trace coincided with the epicentral distribution of both the main shock and the aftershocks.

The analysis of the focal mechanism showed that the main shock could be broken down to three sub-events, located on a rupture plane of NE average trend (Kikuchi,1995; Sato *et al.*, 1996; Wald, 1996). The first two events were spaced 9 km apart and the third one was 4 km away from the second. The total rupture time was 11 seconds, with the break migrating from SW towards the NE (Figure 5). The migration of the seismic source is held responsible for the significantly high acceleration values measured within the urban complex of Kobe. Specifically, the maximum intensity was I_{EMS92} = XI and acceleration was 833 cm sec^{-2}, respectively (Figure 6) (RCEP-DPRI, 1995). On the other hand, the intensity and acceleration on Awaji did not exceed I_{EMS92} = VII and 200 cm sec^{-2}, respectively (see also Takemiya and Adam 1995, Usami *et al.*, 2000). Additionally, because of the Doppler–Fiseau effect, the oscillation period was much longer on Awaji than in Kobe, a fact reflected in the significant differentiation in damage type and distribution for various building types. In other words, because of the short natural period of the low structures (mostly one- or two-story wooden buildings),

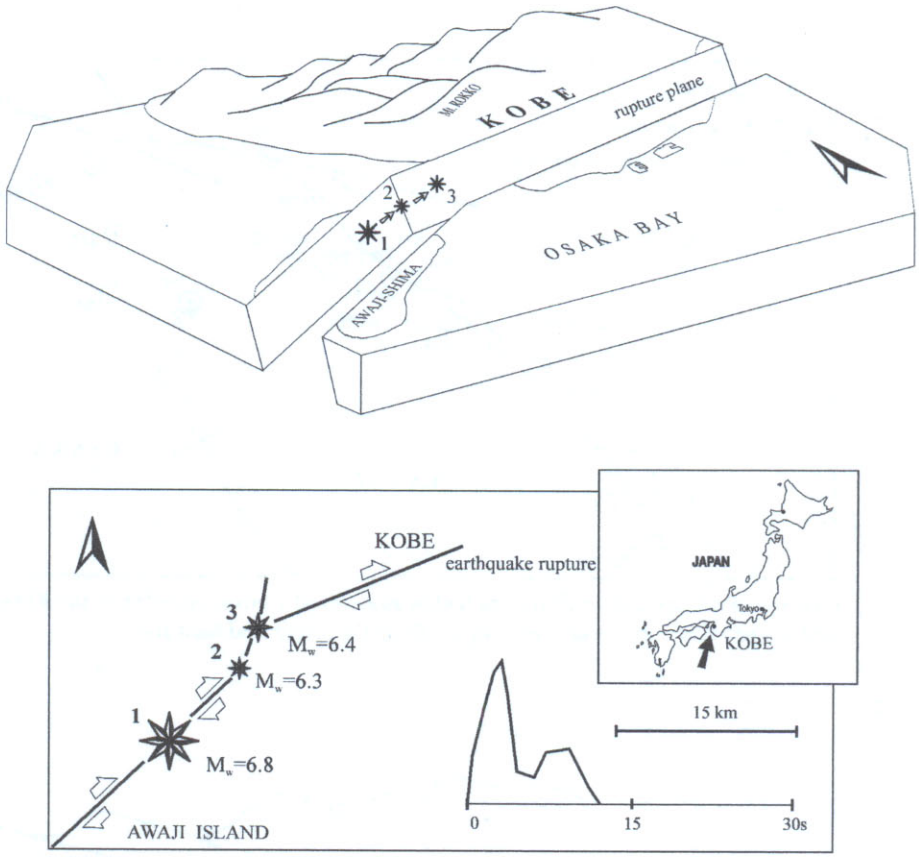

Figure 5. Block diagram to show the migration of the seismic source along the rupture plane in the Kobe earthquake and analysis of earthquake mechanism.

the conditions were more unfavorable in Kobe, as the Doppler–Fiseau effect led to shorter wave periods towards the NE (Kobe) instead of SE (Awaji), which matched the structures' natural period. (Lekkas and Kranis, 1997).

Similar effects of selective distribution of high intensity values along seismic fault traces seemed to have been caused by seismic wave convergence, a result of migration of the earthquake focus in the Dinar earthquake. The surface rupture in this event had an average NW-SE trend, a length of 11 km, maximum displacement of 40 cm and kinematic characteristics that coincide with the earthquake focal mechanism solution (Carydis *et al.*, 1995b; Lekkas, 1998). The fault ran through the urban areas of Yapaqli, Kizilli, Yakakoy and Dinar, all of which were located (from NW-SE to SE) along the foot of a NW-SE elongated mountainous mass (Figure 7).

The most severe damage (and highest intensities) were observed in Dinar, reaching I_{EMS92} = X at the southeastern portion of the fault. At the same location, modern low- or high-rise buildings, usually earthquake-proof, collapsed or suffered con-

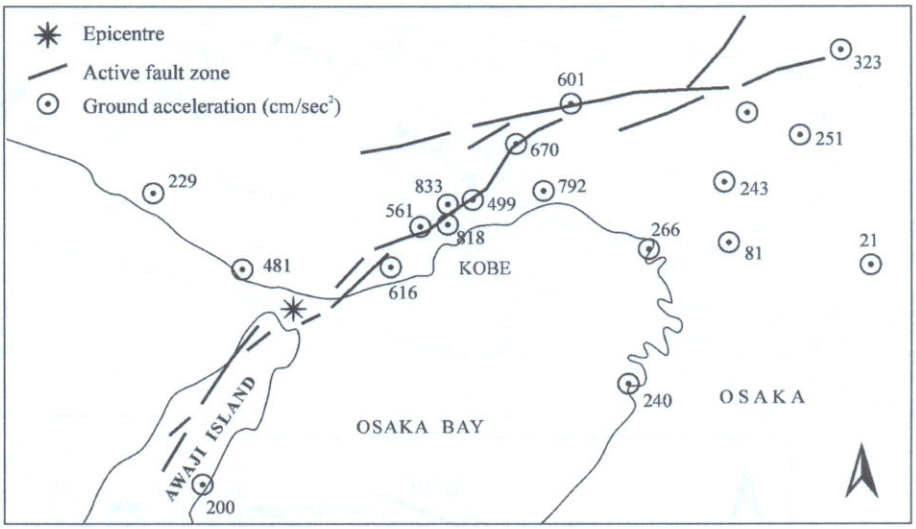

Figure 6. Peak ground accelerations within Kobe–Osaka urban complex in the Kobe earthquake. The values are significantly higher along the reactivated fault zone.

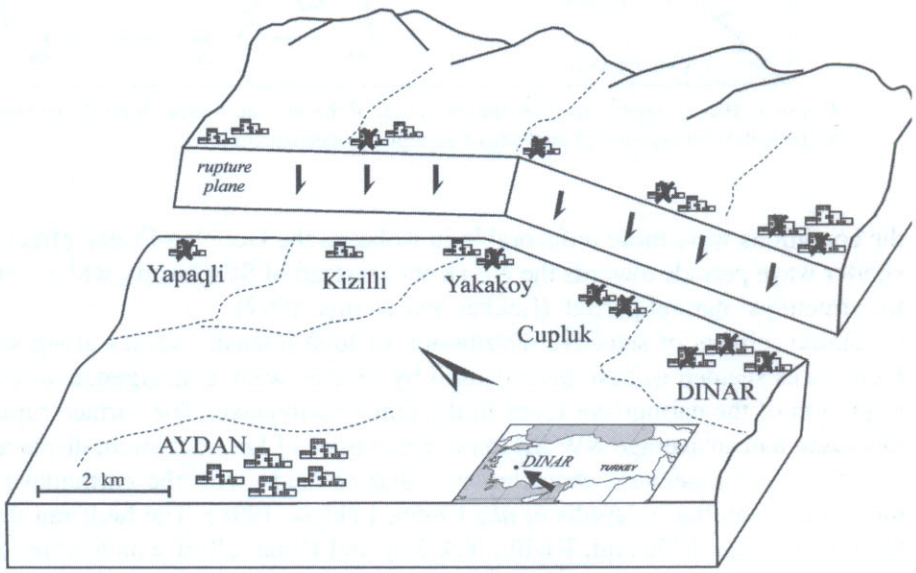

Figure 7. Block diagram to show the reactivated fault in the 1 October 1995 Dinar earthquake. Damage increased gradually along the fault trace and towards Dinar, where the highest intensity values were recorded.

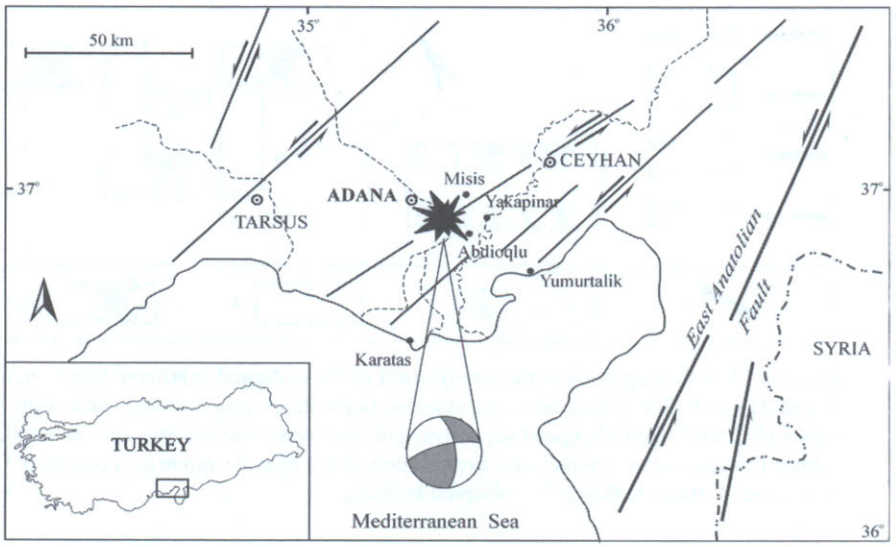

Figure 8. Sketch map showing the epicentre, focal mechanism solution and the dominant fault grain in the broader area of Adana. Ceyhan lies to the northeast of the epicentre, along a reactivated fault zone.

siderable damage. On the other hand, towards the NW and at Cupluk, Yakakoy, Kizilli and Yapaqli, the intensities gradually decreased and relatively old buildings were damaged. It is therefore considered certain that the gradual SE-ward increase of intensity values was due to the migration of the earthquake focus towards this direction.

5. Azimuthal Location and Morphology of Constructions

A special case of damage inflicted on multistory buildings was observed in Ceyhan during the Adana earthquake, which hit severely the broader area. The earthquake epicentre lay at the southern suburbs of Adana and the reactivated faults had a NE-SW trend, consistent with the earthquake focal mechanism (Figure 8).

The city of Ceyhan lies approximately 45 km NW of Adana and is inhabited by 80 000 people. The urban landscape comprises a wide variety of constructions, in terms of construction type, age, building volume and use. Besides the massive damage, which was, to a degree, expected because of the age and quality of constructions, there were a few noticeable cases at the eastern part of the city. There, the most prominent buildings are six- to eight-story apartment blocks, built to meet earthquake design criteria according to the local authorities (Figure 9).

More specifically, a series of twenty rectangular-based apartment blocks, used for housing purposes have been built at the eastern sector of the city. All of them are identical in type and form, but are oriented in two different ways. Half of them

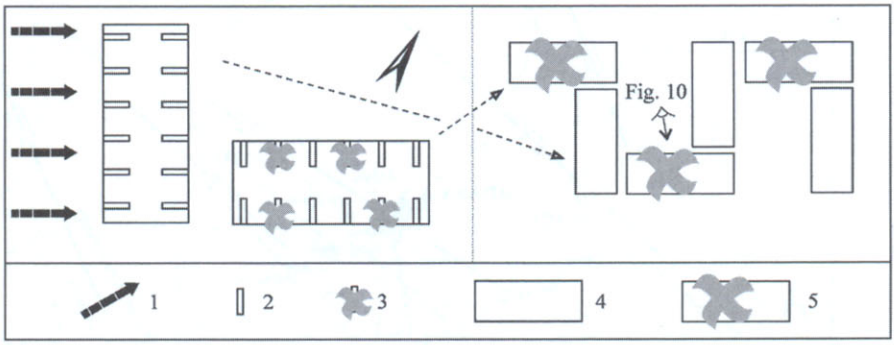

Figure 9. Simple map to show the arrangement of the collapsed apartment blocks in Ceyhan. The collapsed buildings had their long side parallel to the propagation direction of the seismic waves (NE-SW); their elongated supporting columns were oriented perpendicular to this direction. 1. Direction of seismic wave propagation. 2. Elongated supporting column. 3. Column that failed. 4. Intact building. 5. Collapsed building.

are oriented along the NE-SW direction and the other half is perpendicular to the former, oriented NW-SE. Among the striking features of those buildings were the elongated supporting columns, whose long side was perpendicular to the long side of the building (Figure 9), that is to say, NE-SW supporting columns for the NW-SE oriented apartment blocks and vice versa.

Of all the apartment blocks, the ones that collapsed were those oriented NE-SW (with NW-SE supporting columns). On the contrary, no collapse was observed at the NW-SE oriented buildings (with NE-SW supporting columns) (Figure 10). This was due to (i) the orientation of the long side of the buildings in relation to the epicentre and (ii) the increased strength of the elongated supporting columns along the direction parallel to their long side. The ones that were oriented parallel to the direction of the seismic wave propagation withstood the shock while the others did not. Finally, it should be noted that within the broader area and in different azimuthal directions (Figure 8) in respect to the epicentre (Tarsus, Yumurtalik, Karatas, etc.), earthquake-induced damage was not significantly increased. This fact underlines the decisive impact of the reactivated NE-SW trending zone on the distribution of damage.

6. Discussion – Conclusions

The aforementioned earthquakes and the damage caused have been valuable sources of information and data, which, if properly exploited, can serve in the earthquake-proof design of urban complexes and constructions. Based on these earthquake events, a number of comments can be made, as to the influence of the effects mentioned in the preceding paragraphs.

Firstly, the fact that there is a rapid increase in intensity along surficially reactivated faults; the most striking examples are those of the Pyrgos, Dinar and

Figure 10. View of the NE-SW oriented apartment blocks that collapsed, with the NW-SE ones having remained relatively intact. Also shown the longitudinal arrangement of the supporting columns. At different azimuth, in respect to the epicentre, damage was quite less, a fact confirming the decisive role of the trend of the reactivated fault zone (NE-SE) in the distribution of damage (Figure 8).

Egio earthquakes. In all these cases, there has been a clear correlation between the geographical distribution of intensities with the size and focal mechanism of the shock, the epicentral location, the length and type of seismic faulting and so forth.

Important, but somewhat unclear, seems to be the role of soil liquefaction, especially along, or very close to the traces of reactivated faults. The coexistence of surficial faulting and liquefaction must be decisive in the occurrence of extensive damage, even at earthquake-proof constructions; representative example is the Egio earthquake.

Another important factor is the effect of seismic wave directivity, caused by migration of the earthquake focus along the rupture plane. This may lead to excessive seismic loading which at times cannot be accommodated even by well designed constructions, as happened in the Kobe and Dinar earthquakes.

Finally, important role is played by the azimuthal location of housing complexes, the type of construction, the shape, volume and construction details in respect to the epicentral location, faulting type and focal mechanism. A representative example of such interplay was the Adana earthquake.

References

Carydis, P., Holevas, K., Lekkas, E. and Papadopoulos, T.: 1995a, The Egion, Greece, Earthquake of June 15, 1995, *EERI Newsletter*, Special Earthquake Report, July 1995, Vol. 29, No. 7, California, pp. 1–3.

Carydis, P., Lekkas, E., Ersoy, U., Uzumeri, S. M., Ozcebe, G., Polat, U., Tankut, T. and Erdik, M.: 1995b, The Dinar, Turkey, Earthquake of October 1, 1995b, *EERI Newsletter*, Special Earthquake Report, November 1995, Vol. 29, No. 11, California, pp. 1–8.

EERC (Earthquake Engineering Research Center): 1995, Geotechnical reconnaissance of the effects of the January 17, 1995, Huogoken-Nanbu earthquake, Japan. Report No. UCB/EERC-95-101, University of California, Berkeley.

Kawase, H.: 1996, The cause of the damage belt in Kobe: The basin-edge effect, constructive interference of the direct S-wave with the basin – induced diffracted/Rayleigh waves, *Seismol. Res. Lett.* **67**(5), 25–34.

Kawase, H., Matsushima, S., Graves, R. and Sommerville, P.: 2000, Strong motion simulation of Hyogo-ken Nanbu (Kobe) earthquake considering both the heterogeneous rupture process and the 3-D basin structure, 12WCEE, Paper No. 0990, New Zealand, 8 pp.

Kikuchi, M.: 1995, Teleseismic analysis of the Southern Hyogo (Kobe), Japan, earthquake of January 17, 1995, Note No. 38, University Seismological, Yokohama City.

Kohketsu, K.: 1995, Are predominant period contents of strong-motions the major cause of severe damage by the Kobe earthquake?, *Monthly Journal of Science* (Kagaku Asahi) **652**, 11–14.

Lekkas, E.: 1996, Pyrgos earthquake damages (based on E.M.S.-1992) in relation with geological and geotechnical conditions, *Soil Dynamics and Earthquake Engineering* **15**, 61–68.

Lekkas, E., Kranis, Ch., Stylianos, P. and Leounakis, M.: 1996a, Brittle tectonics: A factor in the intensity distribution of the Hanshin earthquake, in *11th World Conference on Earthquake Engineering*, Paper No. 143, Elsevier Science Ltd., Acapulco.

Lekkas, E., Lozios, S., Skourtsos, E. and Kranis, Ch.: 1996b, Liquefaction, ground fissures and coastline change during the Egio earthquake (15 June 1995; Central-Western Greece), *Terra Nova*, **8**(6), 648–654.

Lekkas, E. and Kranis, H.: 1997, The Doppler–Fiseau effect on the damage distribution during the Kobe earthquake (Japan), in *Earthquake Resistant Engineering Structures, Advances in Earthquake Engineering*, Vol. 2, Computational Mechanics Publications, pp. 57–66.

Lekkas, E., Lozios, S., Kranis, H. and Skourtsos, E.: 1997, Linear damage distribution and seismic fractures at the Egio earthquake (15 June 1995, Greece), *Earthquake Resistant Engineering Structures, Advances in Earthquake Engineering*, Vol. 2, Computational Mechanics Publications, pp. 37–46.

Lekkas, E., Lozios, S., Skourtsos, E. and Kranis, H.: 1998, Egio earthquake (15 June 1995): An episode in the neotectonic evolution of Corinthiakos gulf, *J. Geodynamics* **26**(2–4), 487–499.

Lekkas, E.: 1998, Dinar earthquake (Turkey, 1st October 1995) correlation of the recent seismicity data and the neotectonic setting in SW Turkey, in *8th Intern. Congress Geol. Soc. Greece 1998, Bull. Geol. Soc. Greece, XXXII/1*, Patra, pp. 199–207.

RCEP (Research Centre for Earthquake Prediction) DPRI: 1995, A preliminary report of investigations on Southern Hyogo Prefecture Earthquake, *DPRI-Kyoto University Newsletter*, Special Issue, pp. 1–8.

RGAFJ (The Research Group for Active Faults in Japan): 1991, *Maps of Active Faults in Japan with Explanatory Text*, University of Tokyo Press, Hongo, Bunkyo-ku, Tokyo 113, Japan.

Sato, T., Kiyono, J. and Toki, K.: 1995, Strong ground motion during the 1995 Hyogo-ken Nambu earthquake, *The Kobe Earthquake: Geodynamic Aspects, Advances in Earthquake Engineering*, Vol. 1, Computational Mechanics Publications, pp. 17–38.

Sato, T., Kiyono, J. and Toki, K.: 1996, Strong ground motion during the 1995 Hyogo-ken Nanbu earthquake, in C. A. Brebbia (ed.), *The Kobe Earthquake: Geodynamical Aspects, Advances in Earthquake Engineering*, Chapter 2, Wessex Institute of Technology, Southampton, UK, pp. 17–38.

Sommerville, P.: 1995, Kobe earthquake: An urban disaster, *EOS* **76**, 49–51.

Takemiya, H. and Adam, M.: 1995, Why the heaviest damages occurred in Kobe during the Huogo-ken Nanbu earthquake, Japan, 1995, in *The Kobe Earthquake: Geodynamic Aspects, Advances in Earthquake Engineering*, Vol. 1, Computational Mechanics Publications, pp. 39–58.

Usami, M., Teshigawara, M., Kitagawa, Y. and Kawase, H.: 2000, Estimation of strong ground motion and building damage in the 1995 Hyog-ken Nanbu earthquake, 12 WCEE, New Zealand, Paper No. 2038, 7 pp.

Wald, D. J.: 1996, Slip history in the 1995 Kobe, Japan earthquake, determined from strong motion, teleseismic and geodetic data, *J. Phys. Earth* **44**, 489–503.